J Neurophysiol 99: 1545–1553, 2008.
First published January 2, 2008; doi:10.1152/jn.00929.2007.

Two-Photon Excitation of Potentiometric Probes Enables Optical Recording of Action Potentials From Mammalian Nerve Terminals In Situ

Jonathan A. N. Fisher,[1] Jonathan R. Barchi,[2] Cristin G. Welle,[3] Gi-Ho Kim,[3] Paul Kosterin,[3] Ana Lía Obaid,[3] Arjun G. Yodh,[1] Diego Contreras,[3] and Brian M. Salzberg[3,4]

[1]*Department of Physics and Astronomy, University of Pennsylvania School of Arts and Sciences, Philadelphia;*
[2]*Department of Bioengineering, University of Pennsylvania School of Engineering and Applied Science, Philadelphia; and* [3]*Departments of Neuroscience and* [4]*Physiology, University of Pennsylvania School of Medicine, Philadelphia, Pennsylvania*

Submitted 17 August 2007; accepted in final form 2 January 2008

Fisher JA, Barchi JR, Welle CG, Kim G-H, Kosterin P, Obaid AL, Yodh AG, Contreras D, Salzberg BM. Two-photon excitation of potentiometric probes enables optical recording of action potentials from mammalian nerve terminals in situ. *J Neurophysiol* 99: 1545–1553, 2008. First published January 2, 2008; doi:10.1152/jn.00929.2007. We report the first optical recordings of action potentials, in single trials, from one or a few (~1–2 μm) mammalian nerve terminals in an intact in vitro preparation, the mouse neurohypophysis. The measurements used two-photon excitation along the "blue" edge of the two-photon absorption spectrum of di-3-ANEPPDHQ (a fluorescent voltage-sensitive naphthyl styryl-pyridinium dye), and epifluorescence detection, a configuration that is critical for noninvasive recording of electrical activity from intact brains. Single-trial recordings of action potentials exhibited signal-to-noise ratios of ~5:1 and fractional fluorescence changes of up to ~10%. This method, by virtue of its optical sectioning capability, deep tissue penetration, and efficient epifluorescence detection, offers clear advantages over linear, as well as other nonlinear optical techniques used to monitor voltage changes in localized neuronal regions, and provides an alternative to invasive electrode arrays for studying neuronal systems in vivo.

INTRODUCTION

The basic unit of information in the nervous system is the fast, all-or-nothing millisecond-scale propagating wave of membrane depolarization termed the action potential (AP). At this fundamental digital level, signal averaging can rarely be used to study the dynamics of neuronal communication and AP timing synchronization, especially when recording spontaneous activity. Such measurements have long been dominated by electrode technology, which is invasive, and limited in spatial resolution. Although the most advanced electrode arrays (Heer et al. 2007; Patolsky et al. 2006) can resolve membrane potential dynamics at multiple sites with micrometer-scale spatial resolution, they require careful interfacing with neuronal preparations and are not capable of recording at different depths within thick samples. Therefore development of techniques capable of single-trial detection of fast, discrete electrical events at single-cell resolution is crucial.

Imaging techniques employing potentiometric dyes as molecular indicators of membrane voltage (Cohen and Salzberg 1978; Salzberg 1983) permit noninvasive measurements of electrical activity from a wide range of excitable structures ranging from individual dendritic spines (Nuriya et al. 2006) to intact, complex neuronal circuits, in vitro as well as in vivo, with extremely high (≤0.002 ms at room temperature) temporal resolution (Salzberg et al. 1993). Previous voltage-sensitive dye imaging of neuronal networks in vitro (e.g., Ang et al. 2005; Contreras and Llinás 2001; Obaid et al. 1999, 2005) and in vivo (e.g., Civillico and Contreras 2006; Fisher et al. 2004; Petersen et al. 2003) have used conventional one-photon (linear) excitation. Although one-photon fluorescence microscopy can be used to measure neuronal activity with high signal-to-noise (S:N), these measurements inherently integrate the activity encoded by out-of-focus fluorescence signals. This spatial summation of signals complicates the interpretation of fluorescence patterns from thick tissue samples and precludes the detection of potentially localized events such as activity in individual nerve terminals and dendrites.

Nonlinear optical microscopy techniques such as two-photon microscopy (Denk et al. 1990) and second harmonic generation (SHG) microscopy (Campagnola et al. 1999; Hellwarth and Christensen 1974; Nuriya et al. 2006; Sheppard et al. 1977) offer intrinsic optical sectioning at micrometer-scale resolution, virtually eliminating spatial signal summation. However, single-trial measurements of fast electrical events in three-dimensional preparations (as opposed to those in low-density cultured neurons; Kuhn et al. 2004; Sacconi et al. 2006) with appreciable S:N have not yet been achieved using nonlinear optical techniques (Sjulson and Miesenboeck 2007). The small size of one-photon fluorescence changes in response to membrane depolarization, the limited two-photon absorption cross-sections (and, for SHG, 2-photon scattering cross-section) of potentiometric probes, and the constraints on incident light intensity imposed by the need to avoid phototoxicity, all conspire against this goal. In the case of SHG, the nonlinear optical signal propagates primarily in the forward direction, rendering epiillumination measurements (180°) severely shot-noise limited. Furthermore, with the exception of a few studies (Fisher et al. 2005; Millard et al. 2005; Moreaux et al. 2003), the wavelength-dependence of potentiometric, nonlinear optical signals has not been explored.

The neurohypophysis (or posterior pituitary) is a classic in vitro preparation for studying evoked release of peptide hormones (Douglas 1973). Magnocellular neurons, with their cell bodies in the hypothalamus, project their axons as a bundle

Address for reprint requests and other correspondence: B. M. Salzberg, Dept. of Neuroscience, Univ. of Pennsylvania School of Medicine, 234 Stemmler Hall, Philadelphia, PA 19104-6074 (E-mail: bmsalzbe@mail.med.upenn.edu).

The costs of publication of this article were defrayed in part by the payment of page charges. The article must therefore be hereby marked "*advertisement*" in accordance with 18 U.S.C. Section 1734 solely to indicate this fact.

of fibers through the median eminence and infundibular stalk, to terminate in the neurohypophysis where they ramify extensively. In the rat, ~20,000 neurons give rise to ~40,000,000 terminals and secretory swellings, each 1–10 μm in diameter, which account for ~99% of the excitable membrane in the neurohypophysis, whereas the short axons contribute only ~1% (Nordmann 1977). When this in vitro preparation is stained with voltage-sensitive dyes and is stimulated electrically, it generates large optical signals. These compound responses, i.e., changes in one-photon absorption (Gainer et al. 1986) or fluorescence (Muschol et al. 2003), represent the synchronous firing of APs from a large population of neurosecretory terminals.

Here we present single-trial two-photon imaging of APs from either individual, or a very few (1–2 μm), nerve terminals in a surgically excised, intact mouse neurohypophysis stained with the naphthyl styryl-pyridinium potentiometric probe di-3-ANEPPDHQ (Obaid et al. 2004). To optimize the recording conditions, we studied the wavelength dependence of the signal with excitation between 800 and 900 nm and emission between 490 and 700 nm. The best two-photon single-trial measurements exhibited high S:N (up to 5:1) and large fractional fluorescence changes (up to ~10%). To our knowledge, these are the first single-trial optical recordings of electrical activity at submicrometer resolution from an intact mammalian preparation using epifluorescence detection, and they provide the methodological foundation for in-depth optical recording of electrical activity from neuronal circuits in vivo.

METHODS

Two-photon imaging optics

To record electrical activity from small nerve terminals in the intact neurohypophysis, we used a home-built two-photon microscope (Fisher 2007). The excitation source was a mode-locked Titanium:Sapphire (Ti:Al_2O_3) laser (Chameleon, Coherent, Santa Clara, CA). Two-photon absorption-induced fluorescence was collected in the epifluorescence path by the objective and redirected to a photomultiplier (PMT) using a dichroic mirror [90% reflectance (R) at 700 nm] followed by an emission filter (typically interference-coated glass absorption filter). To minimize distortion of the beam profile, we adjusted the average excitation power at the sample to be ~10–20 mW using a $\lambda/2$ plate and a Glan–Thompson polarizer. The PMT used to detect two-photon excited fluorescence was an R943 (Hamamatsu Photonics, Hamamatsu City, Japan) operating in analog mode. (Signals were recorded as analog because the photon flux was too high for reliable photon counting.) To monitor and correct for fluctuations in the square of the laser power ($\langle P(t)\rangle^2$), a small fraction of the beam was picked off with a microscope coverslip and focused onto a β-barium borate (β-BaB_2O_4, or BBO) SHG crystal. This SHG signal was filtered with a BG39 Schott glass absorption filter and detected by an auxiliary PMT (R955, Hamamatsu Photonics), also operating in analog mode. The excitation beam was scanned in the sample plane using galvanometer scanning mirrors from Cambridge Technology (Lexington, MA) and a piezoelectric-driven objective translator (P721, Physik Instrumente, Karlsruhe/Palmbach, Germany) scanned the beam along the vertical (illumination) axis. The combination of scan lens and tube lens allowed us to expand the excitation laser beam and back-fill a microscope objective (×20/0.95 NA XLUMPlanFl, Olympus, Melville, NY). The dichroic mirror that selected the two-photon excited fluorescence emission ($R < 700$ nm), and the various emission interference filters were from Chroma Technology (Rockingham, VT). Analog signals from both PMTs were amplified with a wide bandwidth transimpedance amplifier (13AMP005, Melles Griot, Carlsbad, CA) before digitization by a multifunction data acquisition board (PCI-6052E, National Instruments, Austin, TX). The voltage outputs from our transimpedance amplifiers were oversampled at 150 kHz, and a number of points equal in duration to our integration time were collected and averaged for each sampled point. Device control and data acquisition were performed by custom-written software using the LabVIEW visual programming environment (National Instruments) (Fisher 2007).

Choice of potentiometric probe for optical recording

Di-3-ANEPPDHQ, a chimeric product of di-8-ANEPPS (Bedlack et al. 1992) and RH-795 (Grinvald et al. 1994), has been shown to be less phototoxic than the former and less prone to internalization than the latter (Obaid et al. 2004). Since phototoxicity compromises the physiology of the tissue under study, and internalization increases background fluorescence, thereby diminishing the S:N, the properties of the di-n-ANEPPDHQ dyes (Obaid et al. 2004) are among the most favorable of the potentiometric probes currently available. Di-3-ANEPPDHQ and di-4-ANEPPDHQ have been recently licensed to Invitrogen and are now commercially available (catalog numbers D36801 and D36802, respectively).

One- and two-photon spectroscopy

Absorption and emission spectra for di-3-ANEPPDHQ were measured using octanol as a solvent to approximate the environment of the dye when bound to membrane (Sims et al. 1974). Final sample concentration was $\leq$100 μM. Absorption measurements were performed on a spectrophotometer (Ocean Optics, Dunedin, FL), and excitation and emission spectrum measurements were performed on a spectrofluorometer (DeltaRAM, Photon Technology International). Two-photon excitation cross sections (σ_2 vs. λ) were measured for the di-octyl analog of di-3-ANEPPDHQ in octanol as described previously (Fisher et al. 2005).

Neurohypophysis preparation

The neurointermediate lobe of the pituitary, that is made up of the pars nervosa (neurohypophysis) and pars intermedia, was obtained ($n = 6$), as previously described (Salzberg et al. 1985), from 30- to 60-day-old female CD-1 mice that had been anesthetized by CO_2 inhalation and decapitated in accordance with institutional guidelines. Briefly, the mouse head was pinned to the bottom of a Sylgard-lined dissection dish, and, following removal of the skin, the skull was opened along the dorsal midline and the bone removed bilaterally. Cutting the optic and olfactory nerves allowed caudal deflection of the brain and rupture of the infundibular stalk, leaving the infundibular stump together with the entire pituitary gland attached to the base of the skull. The gland, gently removed using fine forceps and iridectomy scissors, was transferred to a dish containing oxygenated mouse Ringer solution (in mM: 154 NaCl, 5.6 KCl, 1.0 $MgCl_2$, 2.2 $CaCl_2$, 10 glucose, and 20 HEPES, adjusted to pH 7.4 with NaOH) where the anterior pituitary (pars anterior) was separated from the neurointermediate lobe and discarded. The pars intermedia, which consists of a delicate lacework of cells supporting the neurohypophysis, provided a convenient border through which the specimen could be pinned to the Sylgard bottom of a small petri dish (see Fig. 2*A*) while preserving the integrity of the neurohypophysis. The tissue was stained by bathing it for 40 min in a Ringer solution containing 50 μg/ml of the potentiometric probe di-3-ANEPPDHQ together with 0.5% ethanol. (The easy solubility of this dye in ethanol rendered the use of DMSO or any surfactants, including Pluronics or PEG, unnecessary. In our experience, 0.5% ethanol is much less perturbing to the neurohypophysis than these other agents.) After staining, the neurohypophysis was

washed in mouse Ringer solution, which was replaced with newly oxygenated medium every 20–30 min to preserve tissue viability.

Before functional imaging, two-photon anatomical survey images such as that shown in Fig. 2*B* were scanned. Stimulation was achieved using a pair of Teflon-coated Pt-Ir (90–10%) electrodes clasping the infundibular stump and consisted of brief (100–500 μs) shocks delivered through a stimulus isolator. The imaging depth was ~150 μm below the surface of the tissue. The focusing routine consisted of advancing the adjustable stage upward until two-photon fluorescence was detected on the surface of the preparation (either by monitoring photomultiplier voltage or by viewing 2-photon fluorescence by eye). Repeated experiments with stained preparations revealed that locating the preparation surface by eye was consistently accurate to within ~50 μm. After obtaining a surface image of the preparation, the objective was translated downward ~150 μm using the objective translator, which has submicrometer precision and repeatability. Although optical signals could be recorded in response to stimulation from depths between the surface and ~300 μm below the surface, a depth of ~150 μm below the surface was used as the standard imaging depth to keep that factor as constant as possible while varying the experimental parameters of excitation and emission wavelengths. This depth was chosen because it offered reliable tissue viability, avoiding potentially damaged surface tissue, while incurring little blurring caused by scattering.

One- and two-photon action spectra

One-photon action spectrum measurements were generated from the $\Delta F/F$ responses ($n = 10$) to electrical stimulation of the intact neurohypophysis at 18 different wavelengths. Excitation wavelength dependence was measured by varying excitation filters (band-pass) and comparing the peak fluorescence ($\Delta F/F$) responses to APs. Because the peak absorption and emission wavelengths for this dye were narrowly shifted using one-photon excitation compared with two-photon excitation, several dichroic mirror and filter combinations were used to study the excitation wavelength range from 360 to 580 nm. The excitation filters were narrow (10-nm FWHM) band-pass filters centered at each excitation wavelength shown in Fig. 4*A*. The dichroic mirror and emission filter combinations were as follows: from 360 to 440 nm, $R < 450$ nm dichroic and Schott OG455 glass emission filter; from 460 to 510 nm, $R < 515$ nm dichroic and Schott OG530 glass emission filter; from 520 to 580 nm excitation, $R < 585$ nm dichroic and Schott OG590 glass emission filter. Because the system excitation and collection efficiency varied with different filter sets, we measured $\Delta F/F$ instead of S:N as a function of excitation wavelength.

The two-photon action spectrum was generated from the results of two-photon functional recordings at different wavelengths. The excitation laser wavelength was tuned between 800 and 900 nm to study the positive (blue) peak of the action spectrum for di-3-ANEPPDHQ because the corresponding two-photon excitation wavelengths for the negative (red) $\Delta F/F$ peak (see Fig. 4*A*) were beyond the tuning range of our mode-locked Ti:Al_2O_3 laser.

The shape of the one-photon action spectrum (Fig. 4*A*) in the wavelength range that corresponds to our two-photon excitation (i.e., approximately one half of the 2-photon excitation wavelength) predicts that the sign of the two-photon signal should be positive for membrane depolarization. This was confirmed (Fig. 6),because the AP is registered optically as an increase in fluorescence.

Two-photon functional recordings

Two-photon imaging was performed with the custom-built microscope shown in Fig. 1 and consisted of short line-scans (typically ~3 points along a line ~0.5 μm long, as in Fig. 6*A*) integrating for ~100 μs at each point. Each point in the raw data traces (e.g., Fig. 6*D*, unfiltered) represents the average of the approximately three points along the short red line segment. Electrical stimuli (~1–10 mA) were delivered within ~50 ms of the beginning of the line-scan to minimize the effect of photobleaching. When multiple stimuli were delivered (maximum 16 stimuli), the stimulation frequency was 16 Hz. Otherwise, all trials were single-stimulus experiments. The records were 100 ms long with 5-s wait time between trials for single stimuli and 500–1,000 ms long with 1-min wait time between trials for trains of stimuli. Averaging, when needed, was performed off-line using exclusively responses within a single multi-stimulus trial. When signal averaging was used (Fig. 6*C*), the number of averaged spikes is indicated in the corresponding figure legend. For each point scanned in functional recordings, fractional fluorescence ($\Delta F/F$) was calculated by subtracting the baseline, F, from each point in the recording, and dividing by this same background. F, in our experiments, was the average of the first 10 data points in the recording. Functional recording data were filtered as indicated in the corresponding figure legends.

RESULTS

The neurohypophysis consists nearly entirely of the nerve terminals and axonal varicosities of magnocellular neurons. Indeed, these elements constitute ~99% of the excitable membrane in the tissue (Nordmann 1977). The remainder of the tissue consists of short axonal branches, electrically silent pituicytes (glial cells), and capillaries, onto which the nerve terminals secrete the peptide hormones oxytocin and vasopressin. Because the axonal varicosities and nerve terminals represent the only electrically excitable tissue in the organ, there is no postsynaptic electrical activity to confound the interpretation of the optical responses, which, until now, have been recorded as compound APs (Gainer et al. 1986; Muschol et al. 2003; Salzberg et al. 1985). Figure 2*A* is an image (at ×10 magnification) of a mouse neurohypophysis mounted in an experimental chamber, with the stimulating electrodes clasping the infundibular stalk. The optical density of the tissue, reminiscent of brain cortex, shows the difficulty of visualizing small, individual subcellular structures. Two-photon fluorescence microscopy circumvents the blurring effect of scattering, thereby revealing finer anatomical detail. Figure 2*B* shows a two-photon background image, obtained with our microscope, of a mouse neurohypophysis stained with the membrane-impermeant fluorescent potentiometric probe di-3-ANEPPDHQ. Individual neurosecretory terminals in situ as small as 1–2 μm in diameter are clearly identified by their fluorescent profiles. Figure 2*C*, a transmission electron micrograph taken from another mouse neurohypophysis, shows individual terminals packed with dense-core secretory granules. A red blood cell inside a small capillary is also apparent. The dense and tortuous topology of the tissue dictates the need to isolate a very small focal volume for recording of activity.

Choice of optimal two-photon excitation wavelength for di-3-ANEPPDHQ

To optimize the use of di-3-ANEPPDHQ for optical measurements of membrane potential, we first characterized the dye spectral properties in octanol, a solvent that simulates the membrane environment (Fig. 3). Figure 3*A* shows absorption- and fluorescence-excitation spectra, whereas Fig. 3*B* shows fluorescence emission with excitation at 425 or 530 nm. It is evident that fluorescence emission peaks beyond 560 nm.

Since the action spectrum of fluorescent voltage-sensitive dyes, $[\Delta F/F]/\Delta V_m$ vs. λ, where V_m is the transmembrane potential) varies widely between phyla and even species (Ross

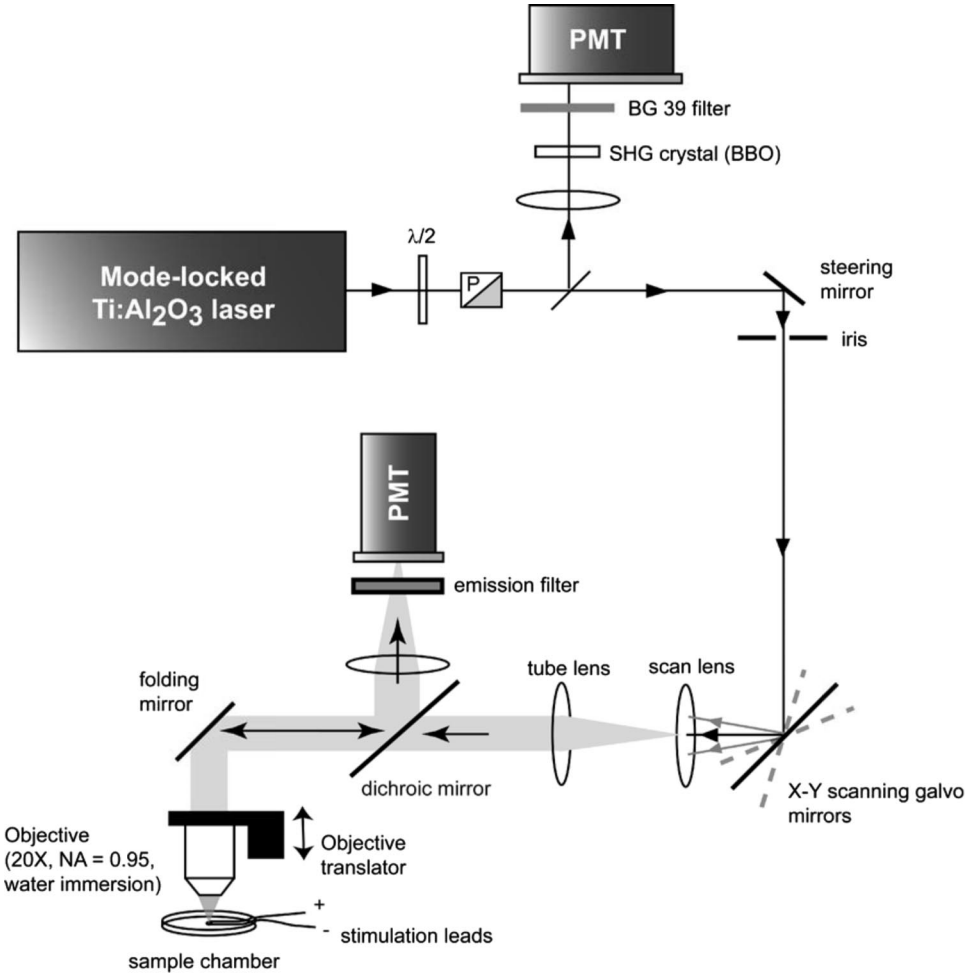

FIG. 1. Optical apparatus for 2-photon imaging and functional recording. The excitation source was a mode-locked titanium:sapphire ($Ti:Al_2O_3$) laser (Chameleon, Coherent). Two-photon absorption-induced fluorescence was collected in the epifluorescence path by the objective and redirected to a photomultiplier (PMT) using a dichroic mirror [90% reflectance (R) at 700 nm] followed by an emission filter. This PMT was an R943 (Hamamatsu Photonics) operating in analog mode. To minimize distortion of the beam profile, the average excitation power at the sample was adjusted to ~10–20 mW using the $\lambda/2$ plate and the Glan–Thompson polarizer (P). The excitation beam was scanned in the sample plane using galvanometer scanning mirrors (Cambridge Technology) and scanned along the vertical (illumination) axis using a piezoelectric-driven objective translator (P721, Physik Instrumente). The combination of scan lens and tube lens expanded the excitation laser beam and back-filled the microscope objective (×20/0.95 NA XLUMPlanFl, Olympus). The dichroic mirror that selected the two-photon excited fluorescence emission ($R < 700$ nm) and the various emission interference filters were from Chroma Technology. To monitor and correct for fluctuations in the square of the laser power [$\langle P(t)\rangle^2$], a small fraction of the beam was picked off with a microscope coverslip and focused onto a β-barium borate (β-BaB_2O_4 or BBO) second harmonic generation (SHG) crystal. This SHG signal was filtered with a BG39 Schott glass absorption filter and detected by a second, auxiliary, PMT (R955, Hamamatsu Photonics) also operating in analog mode.

and Reichardt 1979), it was important to characterize it for di-3-ANEPPDHQ in the mouse neurohypophysis. (It should be noted, here, that the AP in mammalian neurohypophysial terminals is known to be ~100 mV; Jackson et al. 1991). Figure 4*A* shows that, when bound to the outer leaflet of the lipid bilayer (bath application), this probe exhibits a biphasic one-photon fluorescence action spectrum. Indeed, in response to depolarization, it shows a prominent decrease in $\Delta F/F$ at ~525 nm (the wavelength customarily used for 1-photon excitation measurements of V_m) and a smaller increase at ~400 nm. The sign change occurs because the absorption spectrum of di-3-ANEPPDHQ is blue-shifted in response to depolarization. Thus ΔF, in response to excitation near the absorption peak, can be either positive or negative, depending on whether the excitation wavelength is on its rising or falling edge.

Optical recording of membrane potential using two-photon fluorescence requires that the molecular probe exhibits a significant $(\Delta F/F)/\Delta V_m$ and possesses an appreciable two-photon excitation cross-section (σ_2). We have previously measured σ_2 (Fisher et al. 2005) as a function of excitation wavelength (λ), for the di-octyl analog of di-3-ANEPPDHQ, and this is shown in Fig. 4*B*. Note the significant cross-section between 780 and 870 nm and note further the rise to 920 nm and, presumably, beyond. The combination of the one-photon fluorescence action spectrum (Fig. 4*A*) and the two-photon excitation cross-section (Fig. 4*B*) might suggest that excitation at 920 nm or beyond would be optimal for two-photon fluorescence measurement of membrane potential in the mouse neurohypophysis. However, there are two important caveats. First, the maximum value of the measured σ_2 coincides with twice the zero-crossing wavelength (460 nm) of the action spectrum, at which $(\Delta F/F)/\Delta V_m$ is near zero (Fig. 4*A*). Second, H_2O absorption in tissue rises dramatically between 920 and 970 nm and does not fall off until ~1.025 μm (Collins 1925), beyond the range of our mode-locked $Ti:Al_2O_3$ laser. To circumvent these obstacles within the limitations imposed by our light

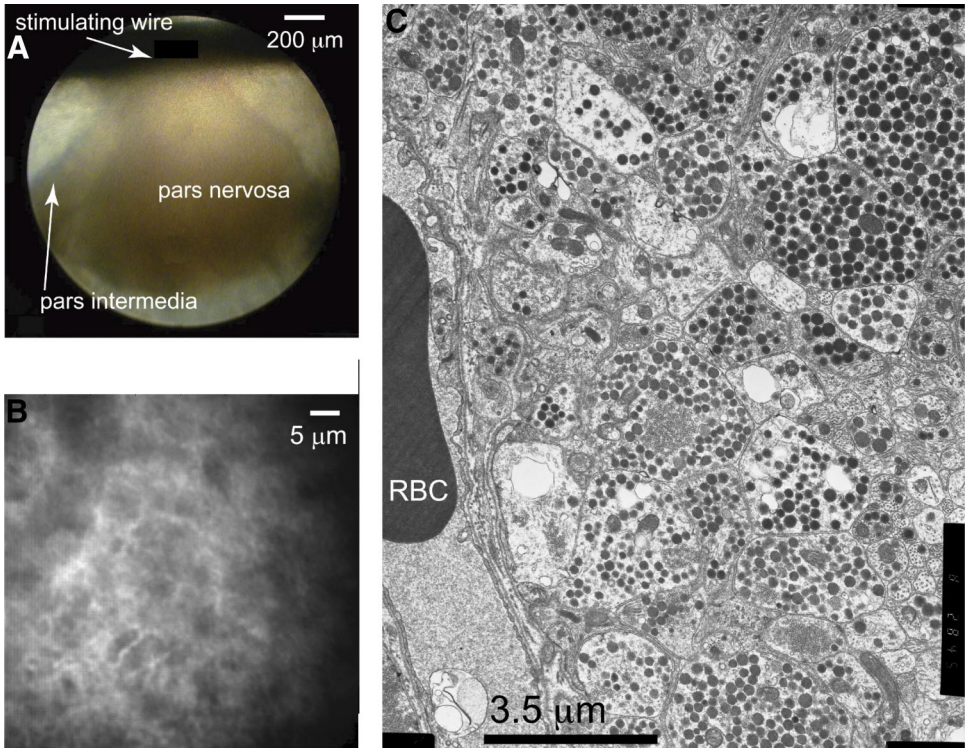

FIG. 2. Anatomy of the neurohypophysis. *A*: dissection microscope image of an isolated neurohypophysis with surrounding pars intermedia and infundibular stalk connecting to stimulation leads (scale bar = 200 μm). *B*: 2-photon background image of neurohypophysis stained with the voltage-sensitive potentiometric probe di-3-ANEPPDHQ. Excitation wavelength = 850 nm. *C*: transmission electron microscope image of mouse neurohypophysis. Individual axon terminals contain peptide hormone-filled vesicles. A red blood cell (RBC) provides scale (diameter ~5.5 μm).

source, we decided to exploit the "blue" peak of the dye's action spectrum and excite di-3-ANEPPDHQ at 850 nm. The two-photon sensitivity of the measurement should depend on the derivative of the cross-section with respect to wavelength (Pons and Mertz 2006), so exciting beyond the 920-nm peak, where the cross-section decreases could, in principle, make sense. However, we were unable to record reliably voltage signals at 955 nm. (As an aside, longer wavelength Ti:Al_2O_3 lasers are now available that reach the local minimum in H_2O absorption at ~1.06 μm, exactly twice the wavelength of the "red" peak in the 1-photon action spectrum.)

Figure 5*A* compares the $\Delta F/F$ of the two-photon excitation action spectrum of di-3-ANEPPDHQ in response to an AP in the neurohypophysis (top *x*-axis), with the $\Delta F/F$ at the "blue" peak of the one-photon action spectrum (bottom *x*-axis). There appears to be a peak in the $\Delta F/F$ response at 850 nm, but it is not statistically significant. Furthermore, the main statistical trend is a downward slope toward 900 nm. S:N is a more relevant experimental parameter than $\Delta F/F$. With that in mind, the same two-photon excitation data are replotted in Fig. 5*B* as S:N. While there was significant statistical variability in single-trial two-photon measurements, a local maximum at 850 nm could be identified. Assuming constant laser intensity over the excitation spectrum, Fig. 5*B* is consistent with both Figs. 5*A* and 4*B*, as the signal-to-noise is proportional to $\Delta F/F$ and the square root of the two-photon excitation cross-section, σ_2, i.e., $S/N \propto (\Delta F \cdot \sqrt{\sigma_2})/F$. The statistical variability in the response is reflected in the error bars in the two-photon action spectra (Fig. 5). Error bars on the one-photon action spectra are significantly smaller, reflecting the fact that those optical responses were

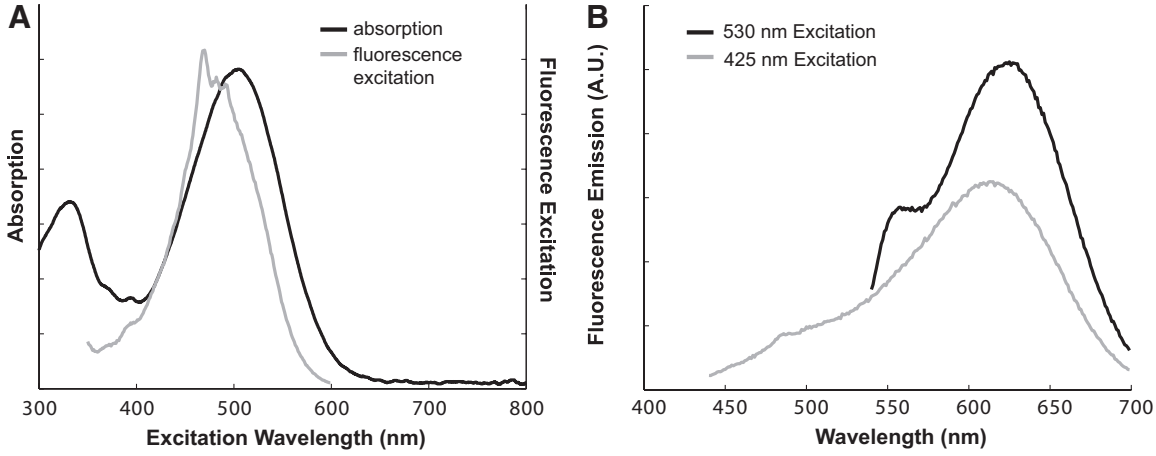

FIG. 3. One-photon spectroscopic data for di-3-ANEPPDHQ. *A*: comparison of absorption (black) and excitation spectrum (gray), which measured fluorescence emission at 610 nm as a function of excitation wavelength (arbitrary units). *B*: fluorescence emission in response to 425- (gray) and 530-nm excitation (black).

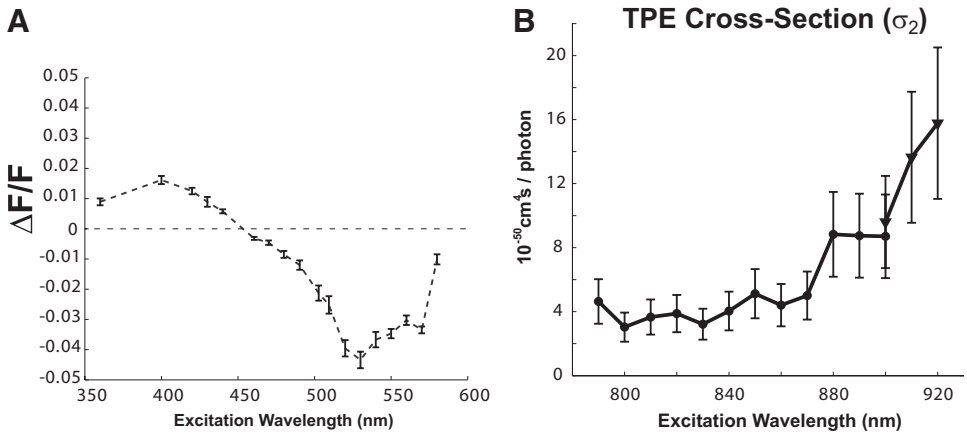

FIG. 4. Spectral measurements of di-3- and di-8-ANEPPDHQ. *A*: 1-photon action spectrum of di-3-ANEPPDHQ. *B*: measured 2-photon excitation cross-sections as a function of excitation wavelength for the voltage-sensitive dye di-8-ANEPPDHQ (data from Fisher et al. 2005).

measured from the entire neurohypophysis and, as such, represent the synchronous firing of hundreds of thousands, if not millions of terminals.

Choice of optimal emission wavelength for two-photon excitation of di-3-ANEPPDHQ

When di-3-ANEPPDHQ is excited at 425 nm, the one-photon fluorescence emission spectrum, measured in octanol, has a peak at ~613 nm and extends much further into the red (Fig. 3*B*). In the stained neurohypophysis, however, with two-photon excitation between 800 and 900 nm, we determined empirically that the optimal wavelength for detecting voltage-dependent changes in fluorescence was ~530 nm. Indeed, band-pass filters centered at longer wavelengths, as well as long-pass filters, yielded measurements with significantly smaller S:N (Fig. 5*B*).

Two-photon optical recording of APs

The results shown in Fig. 6 establish the two-photon technique as a valuable tool for optical recording of electrically evoked APs from individual, or, at most, a very few (see DISCUSSION) nerve terminals in situ, using a voltage-sensitive dye. Figure 6*A* shows the two-photon background image and the recording location from which the data in Fig. 6, *B* and *C*, were obtained. Functional imaging consisted of short line-scans (typically ~3 points along a line ~0.5 μm long, as seen in the inset of Fig. 6*A*) integrating for ~100 μs at each location. Each point in the final data traces (e.g., Fig. 6, *B* and *D*) represents the average of approximately three points along the short (red) line (line scanning was used instead of static single-point "beam-parking" to minimize phototoxicity).

Figure 6*B* shows a train of APs (16 stimuli delivered at 16 Hz) recorded optically, in a single trial, from the location indicated in red in Fig. 6*A*. Figure 6*C* shows the spike-average of the 16 optical responses from the single trial shown in Fig. 6*B*. The characteristic shape of the neurohypophysial AP (Gainer et al. 1986; Muschol et al. 2003), including its after-hyperpolarization, is clearly visible. Figure 6*D* shows a single-trial recording of an AP from an individual nerve terminal (or, possibly, as many as 4–6 nerve terminals), unfiltered, on the left, and filtered, on the right, and exemplifies the high S:N and large Δ*F*/*F* (~10%/100 mV) achievable with this technology. Single-trial responses were 2–3 ms wide at half-maximum, and

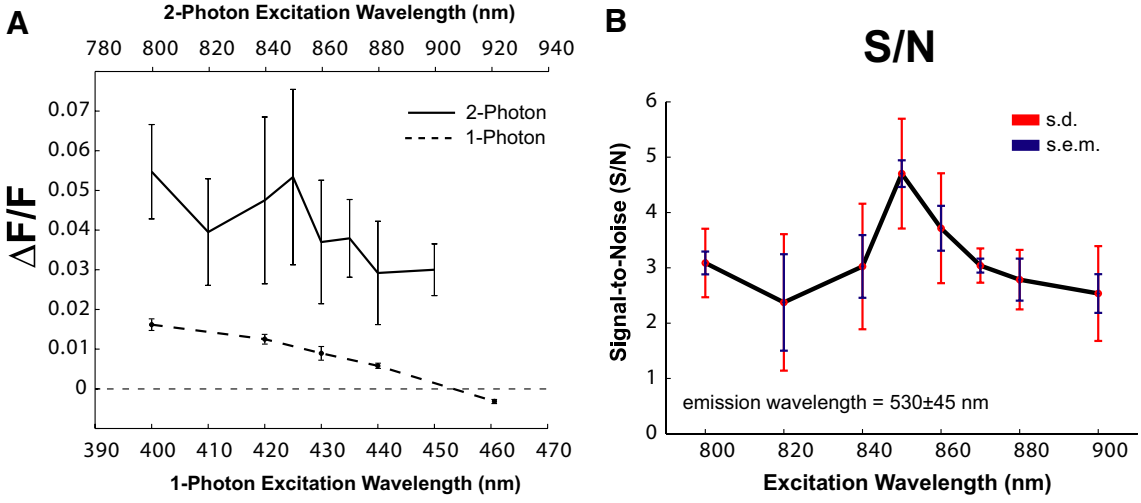

FIG. 5. Comparison of 1- and 2-photon action spectra. *A*: 1- and 2-photon action spectra for di-3-ANEPPDHQ expressed as Δ*F*/*F*. Note that the 2-photon action spectrum is shown on a different scale (top axis) for wavelength comparison. *B*: S:N in 2-photon excited fluorescence signal as a function of excitation wavelength in single-trial optical recordings of action potentials ($n = 10$). Red error bars represent SD; blue bars represent SE. S:N has been defined here as the amplitude of the evoked signal (peak-to-peak) divided by the RMS noise, which is calculated from data recorded before the stimuli were delivered (i.e., 50 ms before).

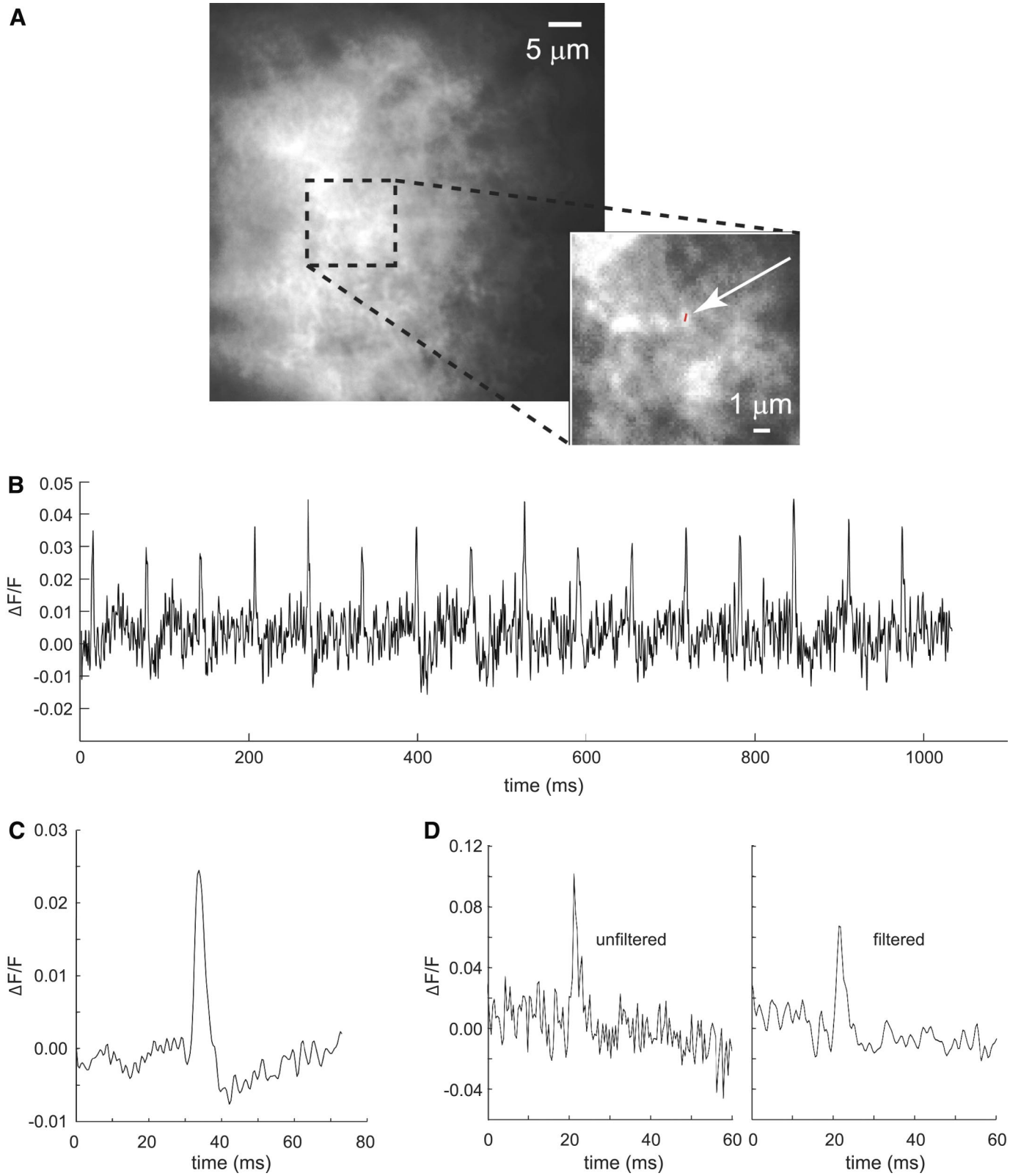

FIG. 6. Functional recording of action potentials from 1, or, at most, a few tightly packed nerve terminals in situ. *A*: background 2-photon image of the region of the neurohypophysis used for functional optical recording (scale = 5 μm). *Inset*: magnified view (scale bar = 1 μm) of imaged region; short red line indicates actual location of line-scan excitation. *B*: single-trial data showing a train of 16 action potentials in response to repeated stimuli delivered at 16 Hz for 1 s. The optical data were band-pass filtered (ideal filter in the frequency domain) between 10 Hz and 0.7 kHz and smoothed using a 3-point sliding boxcar average. *C*: average of the 16 action potentials from the single trial shown in *B*. *D*: single-trial response to an electrical stimulus exhibiting both high S:N and large $\Delta F/F$ (nearly 10%). The trace on the *left* is raw data (unfiltered), and the trace on the *right* is filtered identically to the trace in *B*. Excitation wavelength = 850 nm; emission wavelength = 530 45 nm.

averaged responses were often 4–5 ms wide. This broadening is likely caused by physiological jitter in the timing of the response, since the recordings represent the activity of just a single, or, at most, a very few nerve terminals. As such, these results are the first demonstration of functional two-photon recording with potentiometric probes of electrically evoked APs from micrometer-scale nerve terminals in situ.

DISCUSSION

This work clearly shows our ability to record APs in single trials from ~1 μm patches of neuronal membrane on small nerve terminals in an intact preparation. Indeed, the special morphology of the mammalian neurohypophysis (Nordmann 1977), combined with the spatial resolution inherent in our two-photon microscope, ensures that our signals have their origin in single, or at most four to six neurosecretory terminals or swellings.

Although experimental measurement of the two-photon focal excitation volume in situ is technically challenging, the lateral and axial dimensions of the focal volume can be calculated from high numerical-aperture formulations of the illumination point spread function (IPSF) (Richards and Wolf 1959), which is the three-dimensional illumination intensity distribution. Because two-photon excitation is proportional to the square of the excitation intensity, measures of the lateral and axial widths of $IPSF^2$ such as FWHM and 1/e width of Gaussian fits to the $IPSF^2$ function are effective measures of lateral and axial resolution (Zipfel et al. 2003). For the case of our overfilled 0.95 NA objective at 850-nm excitation, assuming the refractive index of the sample to be ~1.4, the lateral and axial 1/e diameters (FWHM) are ~0.4 and ~1.8 μm, respectively.

Scattering caused by heterogeneities in the tissue refractive index affects both the excitation and fluorescence photon trajectories. In single-point scanning two-photon microscopy, all collected fluorescence is attributed to the focal volume, thus scattering of the fluorescence signal does not affect spatial resolution. Scattering of the illumination photons, however, can cause a portion of the illumination to be deviated from the focal volume, and thus can change the effective focal volume. Because the excitation power used in these experiments was moderate (~10–20 mW) and the two-photon absorption cross-section of the dye was relatively small at the 850-nm excitation wavelength (<10 GM), it is unlikely that scattered (i.e., non-ballistic) excitation photons seriously expanded the focal volume and decreased spatial resolution. Nevertheless, it is certainly reasonable that scattering could have somewhat expanded the focal volume from which the optical recordings were made. Assuming that scattering doubled the 1/e diameters of the $IPSF^2$, the axial and spatial resolutions would be ~0.8 and ~3.6 μm, respectively. If the line scan excitation point intersected an ~1-μm nerve terminal at the interface with another nerve terminal, these expanded resolutions would integrate the virtually synchronous activity of approximately six nerve terminals, as an upper limit. Since care was taken to direct the line scan in the center of nerve terminal fluorescence profiles, however, it is more likely that three or fewer nerve terminals contributed to the fluorescence signal. Finally, assuming that scattering did not lead to such a drastic decrease in axial resolution, it is most probable that the signals shown in Fig. 6 have their origin in the stained membrane of an individual nerve terminal. However, definitive proof that the optical signal reflects the activity of only a single terminal must await further experiments.

Interestingly, two-photon excitation yielded fractional fluorescence changes ~5 times larger than one-photon excited $\Delta F/F$ at corresponding ($\lambda_{2Photon}/2$) excitation wavelengths. Such increases in $\Delta F/F$ following two-photon excitation are consistent with reported measurements in cultured neurons stained with a hemicyanine potentiometric probe (Kuhn et al. 2004). While this agreement may be fortuitous (since these measurements were made using excitation at opposite sides of the absorption spectrum), it is noteworthy, since the relatively poor S:N of one-photon measurements is caused in no small part by the small fractional fluorescence changes exhibited in this mode, and, in light of our study (and that of Kuhn et al. 2004), it seems that two-photon excitation recordings may not be limited in this way.

Although our present apparatus did not permit excitation beyond 960 nm, we recognize that infrared functional two-photon imaging of membrane potential offers exciting possibilities that must be pursued. Obvious advantages include greater penetration into highly scattering tissue and diminished likelihood of photodynamic damage. Previous evidence (our Fig. 4*B*; Fisher et al. 2005) suggests that several voltage-sensitive dyes have the peak of their two-photon absorption cross-sections beyond 960 nm. Since the one-photon action spectrum clearly indicates that larger signals can be expected for two-photon excitation between 1.000 and 1.150 μm, measurement of σ_2 at these longer wavelengths, using newly available mode-locked $Ti:Al_2O_3$ lasers, should permit optimization of the excitation parameters, thereby increasing even further the sensitivity and, by virtue of increased sensitivity, the spatial resolution of the technique.

The large $\Delta F/F$ signals with high S:N described here are particularly relevant to neuroscience and neurology, where the mammalian brain is of primary interest. Even more significant is the fact that this technique uses epifluorescence detection of the optical signals, i.e., detection in the backward direction, a measurement modality that will permit noninvasive recording of electrical activity from intact brain. Furthermore, the fact that the molecular probes are applied in the bath, rather than by intracellular injection of a single neuron (Antic and Zecevic 1995; Djurisic et al. 2004; Grinvald et al. 1987), and that the recording sites are inherently very small by virtue of the properties of the two-photon excitation, means that multiplexing schemes, including laser scanning and multi-beamlet excitation (Crepel et al. 2007; Fisher 2007; Kurtz et al. 2006), will permit optical recording from nerve terminals or dendrites from multiple cells virtually simultaneously.

ACKNOWLEDGMENTS

We thank A. P. Reid, J. Wester, K. Lee, and M. Goulian for useful discussions and A. Callahan for technical assistance.

Present address of J.A.N. Fisher: Howard Hughes Medical Institute and Laboratory of Sensory Neuroscience, The Rockefeller University, New York, NY 10021.

GRANTS

This work was supported by David and Lucille Packard Foundation Grant 2000-01737 and National Institutes of Health Grants NS-16824 and NS-40966 to B. M. Salzberg and EY-13984 to D. Contreras.

REFERENCES

Ang CW, Carlson GC, Coulter DA. Hippocampal CA1 circuitry dynamically gates direct cortical inputs preferentially at theta frequencies. *J Neurosci* 25: 9567–9580, 2005.

Antic S, Zecevic D. Optical signals from neurons with internally applied voltage-sensitive dyes. *J Neurosci* 15: 1392–1405, 1995.

Bedlack RS Jr, Wei M, Loew LM. Localized membrane depolarizations and localized calcium influx during electric field-guided neurite growth. *Neuron* 9: 393–403, 1992.

Campagnola PJ, Wei MD, Lewis A, Loew LM. High-resolution nonlinear optical imaging of live cells by second harmonic generation. *Biophys J* 77: 3341–3349, 1999.

Civillico EF, Contreras D. Integration of evoked responses in supragranular cortex studied with optical recordings in vivo. *J Neurophysiol* 96: 336–351, 2006.

Cohen LB, Salzberg BM. Optical measurement of membrane potential. *Rev Physiol Biochem Pharmacol* 83: 35–88, 1978.

Collins JR. Change in the infra-red absorption spectrum of water with temperature. *Physiol Rev* 26: 771–779, 1925.

Contreras D, Llinás R. Voltage-sensitive dye imaging of neocortical spatiotemporal dynamics to afferent activation frequency. *J Neurosci* 21: 9403–9413, 2001.

Crepel V, Aronov D, Jorquera I, Represa A, Ben-Ari Y, Cossart R. A parturition-associated nonsynaptic coherent activity pattern in the developing hippocampus. *Neuron* 54: 105–120, 2007.

Denk W, Strickler JH, Webb WW. Two-photon laser scanning fluorescence microscopy. *Science* 248: 73–76, 1990.

Djurisic M, Antic S, Chen WR, Zecevic D. Voltage imaging from dendrites of mitral cells: EPSP attenuation and spike trigger zones. *J Neurosci* 24: 6703–6714, 2004.

Douglas WW. How do neurones secrete peptides? Exocytosis and its consequences, including "synaptic vesicle" formation, in the hypothalamo-neurohypophyseal system. *Prog Brain Res* 39: 21–39, 1973.

Fisher JAN. *Linear and Non-Linear Fluorescence Imaging of Neuronal Activity* (PhD thesis). Department of Physics and Astronomy, University of Pennsylvania, Philadelphia, PA, 2007.

Fisher JAN, Civillico EF, Contreras D, Yodh AG. in vivo fluorescence microscopy of neuronal activity in three dimensions by use of voltage-sensitive dyes. *Opt Lett* 29: 71–73, 2004.

Fisher JAN, Salzberg BM, Yodh AG. Near infrared two-photon excitation cross-sections of voltage-sensitive dyes. *J Neurosci Methods* 148: 94–102, 2005.

Gainer H, Wolfe SA Jr, Obaid AL, Salzberg BM. Action potentials and frequency-dependent secretion in the mouse neurohypophysis. *Neuroendocrinology* 43: 557–563, 1986.

Grinvald A, Lieke EE, Frostig RD, Hildesheim R. Cortical point-spread function and long-range lateral interactions revealed by real-time optical imaging of macaque monkey primary visual cortex. *J Neurosci* 14: 2545–2568, 1994.

Grinvald A, Salzberg BM, Lev-Ram V, Hildesheim R. Optical recording of synaptic potentials from processes of single neurons using intracellular potentiometric dyes. *Biophys J* 51: 643–651, 1987.

Heer F, Hafizovic S, Ugniwenko T, Frey U, Franks W, Perriard E, Perriard JC, Blau A, Ziegler C, Hierlemann A. Single-chip microelectronic system to interface with living cells. *Biosens Bioelectron* 22: 2546–2553, 2007.

Hellwarth R, Christensen P. Nonlinear optical microscope examination of structures in polycrystalline ZnSe. *Opt Commun* 12: 318–322, 1974.

Jackson MB, Konnerth A, Augustine GJ. Action potential broadening and frequency-dependent facilitation of calcium signals in pituitary nerve terminals. *Proc Natl Acad Sci USA* 88: 380–384, 1991.

Kuhn B, Fromherz P, Denk W. High sensitivity of Stark-shift voltage-sensing dyes by one- or two-photon excitation near the red spectral edge. *Biophys J* 87: 631–639, 2004.

Kurtz R, Fricke M, Kalb J, Tinnefeld P, Sauer M. Application of multiline two-photon microscopy to functional in vivo imaging. *J Neurosci Methods* 151: 276–286, 2006.

Millard AC, Jin L, Wuskell JP, Boudreau DM, Lewis A, Loew LM. Wavelength- and time-dependence of potentiometric non-linear optical signals from styryl dyes. *J Membr Biol* 208: 103–111, 2005.

Moreaux L, Pons T, Dambrin V, Blanchard-Desce M, Mertz J. Electro-optic response of second-harmonic generation membrane potential sensors. *Opt Lett* 28: 625–627, 2003.

Muschol M, Kosterin P, Ichikawa M, Salzberg BM. Activity-dependent depression of excitability and calcium transients in the neurohypophysis suggests a model of "stuttering conduction". *J Neurosci* 23: 11352–11362, 2003.

Nordmann JJ. Ultrastructural morphometry of the rat neurohypophysis. *J Anat* 123: 213–218, 1977.

Nuriya M, Jiang J, Nemet B, Eisenthal KB, Yuste R. Imaging membrane potential in dendritic spines. *Proc Natl Acad Sci USA* 103: 786–790, 2006.

Obaid AL, Koyano T, Lindstrom J, Sakai T, Salzberg BM. Spatiotemporal patterns of activity in an intact mammalian network with single-cell resolution: optical studies of nicotinic activity in an enteric plexus. *J Neurosci* 19: 3073–3093, 1999.

Obaid AL, Loew LM, Wuskell JP, Salzberg BM. Novel naphthyl styryl-pyridinium potentiometric dyes offer advantages for neural network analysis. *J Neurosci Methods* 134: 179–190, 2004.

Obaid AL, Nelson ME, Lindstrom J, Salzberg BM. Optical studies of nicotinic acetylcholine receptor subtypes in the guinea-pig enteric nervous system. *J Exp Biol* 208: 2981–3001, 2005.

Patolsky F, Timko BP, Yu G, Fang Y, Greytak AB, Zheng G, Lieber CM. Detection, stimulation, and inhibition of neuronal signals with high-density nanowire transistor arrays. *Science* 313: 1100–1104, 2006.

Petersen CC, Grinvald A, Sakmann B. Spatiotemporal dynamics of sensory responses in layer 2/3 of rat barrel cortex measured in vivo by voltage-sensitive dye imaging combined with whole-cell voltage recordings and neuron reconstructions. *J Neurosci* 23: 1298–1309, 2003.

Pons T, Mertz J. Membrane potential detection with second-harmonic generation and two-photon excited fluorescence: a theoretical comparison. *Opt Commun* 258: 203–209, 2006.

Richards B, Wolf E. Electromagnetic diffraction in optical systems II. Structure of the image field in an aplanatic system. *Proc R Soc London A* 253: 358–379, 1959.

Ross WN, Reichardt LF. Species-specific effects on the optical signals of voltage-sensitive dyes. *J Membr Biol* 48: 343–356, 1979.

Sacconi L, Dombeck DA, Webb WW. Overcoming photodamage in second-harmonic generation microscopy: real-time optical recording of neuronal action potentials. *Proc Natl Acad Sci USA* 103: 3124–3129, 2006.

Salzberg BM. Optical recording of electrical activity in neurons using molecular probes. In: *Current Methods in Cellular Neurobiology*, edited by Barker J, McKelvy J. New York: John Wiley, 1983, p. 139–187.

Salzberg BM, Obaid AL, Bezanilla F. Microsecond response of a voltage-sensitive merocyanine dye: fast voltage-clamp measurements on squid giant axon. *Jpn J Physiol* 43: S37–S41, 1993.

Salzberg BM, Obaid AL, Gainer H. Large and rapid changes in light scattering accompany secretion by nerve terminals in the mammalian neurohypophysis. *J Gen Physiol* 86: 395–411, 1985.

Sheppard CJR, Kompfner R, Gannaway J, Walsh D. The scanning harmonic optical microscope. *IEEE J Quant Electron* QE13: 100D, 1977.

Sims PJ, Waggoner AS, Wang CH, Hoffman JF. Studies on the mechanism by which cyanine dyes measure membrane potential in red blood cells and phosphatidylcholine vesicles. *Biochemistry* 13: 3315–3330, 1974.

Sjulson L, Miesenboeck G. Optical recording of action potentials and other discrete physiological events: a perspective from signal detection theory. *Physiology (Bethesda)* 22: 47–55, 2007.

Zipfel WR, Williams RM, Webb WW. Nonlinear magic: multiphoton microscopy in the biosciences. *Nat Biotechnol* 21: 1369–1377, 2003.